The p-Ge Terahertz Laser—Properties Under Pulsed- and Mode-Locked Operation

J. Niels Hovenier, M. Carmen Diez, Tjeerd O. Klaassen, *Associate Member, IEEE*, W. Tom Wenckebach, Andrej V. Muravjov, Sergey G. Pavlov, and Valerie N. Shastin

***Abstract*—The results of a detailed study of the optical output of the p-Ge hot hole terahertz laser for pulsed-locked, as well as for mode-locked operation, is reported in this paper. The recently developed technique to achieve active mode locking is described. Results on the shape of the pulses in the small-signal gain, as well as in the saturated gain regime under mode-locked operation, are given. These will be discussed in the light of new results on time- and wavelength-resolved experiments for normal pulsed operation. Under favorable conditions, it is found that trains of pulses with a full width at half maximum pulsewidth of 100 ps can be produced.**

***Index Terms*—Mode locking, p-Ge hot hole laser, small-signal gain, terahertz radiation.**

I. Introduction

THE p-Ge hot hole laser is as yet the only solid-state laser with a strong and tunable broad-band emission in the terahertz frequency range. A well-known disadvantage of this source is the strong heating of the cryogenically cooled laser crystal, resulting from the particular laser excitation mechanism. As a consequence, only short pulsed operation is possible [1]. Lately, much effort has been put into the development of techniques to realize continuous wave (CW) operation of this laser, in order to enable the use of this source for instance as local oscillator in terahertz heterodyne systems [2]. Recently, duty cycles as high as 2.5% have been obtained, using very small laser crystals doped with *double* acceptors [3], [4]. Until now, however, not much work has been performed to employ the possibilities of this laser to create *very short* pulses that could be of use for time-resolved experiments in which monochromatic terahertz radiation is needed.

Some time ago, a possible method, based on the results of Monte Carlo simulations, was discussed to actively mode lock the p-Ge laser [5]. Using that proposed modulation technique, we recently succeeded in the first experimental realization of mode-locked operation [6],[7]. In this paper, we present results of a study on the relation between wavelength, small-signal gain, and pulseshape on the one hand, and excitation conditions on the other hand, for this pulsed mode-locked laser. Peculiar properties of the optical output of this mode-locked laser appear to be intimately related to the wavelength dependence of gain and pulseshape, as observed for *long pulsed* operation. We show that we are able to produce trains of terahertz pulses with a full width at half maximum (FWHM) width shorter than 100 ps.

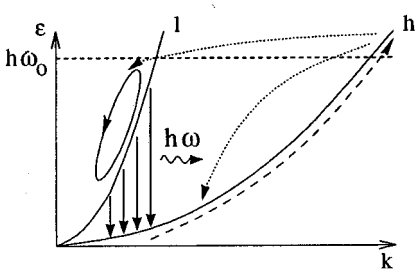

Fig. 1. Mechanism for population inversion in a p-Ge intervalence band laser: light (l) and heavy (h) hole subbands are shown in an energy–momentum diagram. The pumping cycle is indicated.

The operation of the p-Ge hot hole laser is based on the acceleration of holes in $\vec{E} \perp \vec{B}$ fields at $T \leq 20$ K [1]. For the proper ratio of E and B fields, $|E/B| \approx 1.5$ kV/cmT, the heavy holes (HH's) are accelerated up to energies above the optical phonon energy $\hbar\omega \approx 37$ meV and, therefore, strongly scattered by optical phonons. A few percent of these HH's are scattered into the light hole (LH) band. The LH's do not reach the optical phonon energy and, are thus, not scattered, but accumulate on closed trajectories below the optical phonon energy (see Fig. 1). The resulting population inversion between the LH and HH bands lead to stimulated emission in the 1.5–4.2-THz range. It must be noted that both bands are split up in discrete Landau levels by the action of the magnetic field. Due to the very short lifetime of the HH's, combined with the small HH Landau level splitting, resulting from the large effective mass, the HH Landau levels merge to one broad band. Due to the longer lifetime of the LH's and the much larger Landau level (and electron spin-) splitting, the LH band does exhibit a discrete structure. Thus, in fact, population inversion occurs between one or more LH Landau levels and the HH band. By increasing the amplitude of both E and B, the frequency of the laser emission tends to increase. For proper action, $\vec{E}$ and $\vec{B}$ must be accurately perpendicular, as a small component of the electric field $\| \vec{B}$ causes an acceleration of the holes that is not restricted by the action of the Lorentz force. This enables the LH's to gain so much energy that they are *also* scattered by optical phonons. As in that process, part of the LH's are scattered into the HH band, which leads to the destruction of the population inversion. Being a disadvantage for normal laser

Manuscript received March 1, 1999.

J. N. Hovenier, M. C. Diez, T. O. Klaassen, and W. T. Wenckebach are with the Department of Applied Physics, Delft Institute of Microelectronics and Submicrontechnology, Delft University of Technology, 2600 GA Delft, The Netherlands (e-mail: tjeerd@hfwork1.tn.tudelft.nl).

A. V. Muravjov, S. G. Pavlov, and V. N. Shastin are with the Institute for Physics of Microstructures, Russian Academy of Sciences, Nizhny Novgorod 603600, Russia.

Publisher Item Identifier S 0018-9480(00)02525-4.

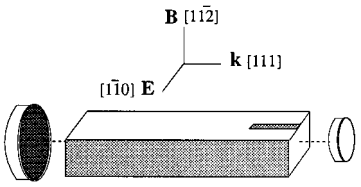

Fig. 2. p-Ge laser cavity design.

operation, this very effect can be employed to obtain a modulation of the laser gain. With the application of a periodic electric field $\vec{E}_\nu \parallel \vec{B}$, the population inversion, and thus, the laser gain reaches a minimum at maximum amplitude of that field, i.e., twice per E_ν cycle. Thus, by choosing the frequency ν equal to *half* the laser cavity round-trip frequency, a modulation of the gain at the round-trip frequency is achieved; the essential prerequisite for active mode locking [5]. The laser sample used (see Fig. 2), the same as in [6], was cut from a single crystal of Ga-doped Ge, with $N_{\rm Ga} = 7.10^{13}$ cm^{-3}, in the form of a rectangular parallelepiped of $a \times b \times l = 5 \times 7 \times 49.46$ mm^3. Two gold mirrors, evaporated on quartz substrates and isolated from the crystal by 10-μm Teflon films, are attached to the ends of the sample, which have been optically polished and made parallel to each other within 30 in. The smaller (4-mm diameter) mirror covers only part of the end face: the laser radiation leaking out alongside this mirror is detected with room-temperature detectors. The high-voltage electric excitation field ($\vec{E} \parallel [1\bar{1}0]$) is applied to ohmic contacts covering two opposite lateral surfaces of the sample in pulses of a few microseconds long to avoid excessive heating. The magnetic field ($\vec{B} \parallel [11\bar{2}]$) is applied perpendicular to the long axis and to $\vec{E}$. The RF field $\vec{E}_\nu \parallel \vec{B}$ for gain modulation is also applied in short pulses, synchronized with the laser excitation, to additional ohmic contacts of 1×10 mm^2 on the (other) lateral sides of the sample. It must be noted that employing the Voigt configuration, i.e., taking the optical axis perpendicular to both $\vec{B}$ and $\vec{E}$, is essential in order to apply the present modulation technique. In the Faraday configuration (optical axis $\parallel \vec{B}$), which is often used to operate the p-Ge laser, the modulation electrodes would block the optical path. As the optical length of the cavity is about $n_{Ge}l$, the laser cavity round-trip frequency equals $c/2n_{Ge}l = 772$ MHz and, thus, the frequency of the modulation field is chosen as $\nu = 386$ MHz.

Fig. 3 gives a schematic overview of the experimental setup. The high-voltage pulser consists of a large low-inductance capacitor bank that can be switched on in two steps. Voltages up to 0.9 kV can be applied to the crystal within 30 ns, using a system of five parallel FET's. To obtain voltages up to 1.8 kV, a prestep is applied using an isolated gate bipolar transistor (IGBT) switch with a rise time of $\leq$500 ns. In this way, the electric field applied to the crystal is always raised within 30 ns from a value far below the active region (see Fig. 3) to the value needed for laser action. The other specifications for this high-voltage pulser are: 1) flatness better than 1% over a 10-μs pulse; 2) $V_{\max} = 1800$ V; 3) $I_{\max} = 500$ A; and 4) output impedance $Z_0 = 4\ \Omega$. A balanced $Z_0 = 4\ \Omega$ transmission line for this high-voltage pulser was made from 75-μm-thick Kapton film with 5-mm-wide copper conductors on both sides. For the gain modulation, a high-voltage proof buffer amplifier

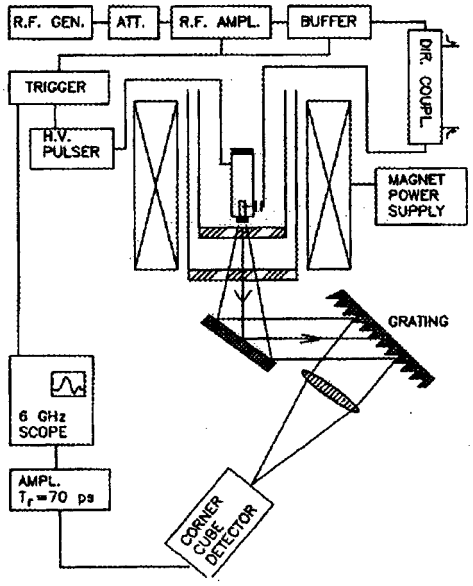

Fig. 3. Schematic view of the experimental setup.

with a 250 W @386 MHz output was developed. The RF power is transferred to the Ge sample by a 50-Ω coaxial cable. Inside the home-build Helium cryostat, as close as possible to the sample, a resonant circuit and transformer are situated to match the $\approx$10-Ω resistance between the RF contacts on the Ge crystal to the 50-Ω cable. The homogeneous electromagnet ($B_{\max} \approx 1.2$ T) with a 65-mm bore, can be rotated to adjust the angle between $\vec{E}$ and $\vec{B}$ to obtain optimum laser action. A z-cut quartz window at the bottom of the cryostat enables an easy outcoupling of the laser radiation. The spectrum of the laser output can be studied with a resolution $\Delta\lambda/\lambda \approx 0.01$ using a 7.9-grooves/mm blazed reflection grating. The optical output is monitored with fast room-temperature GaAs Schottky diode detectors (Faran Technology, Cork, Ireland) and/or slower pyroelectric detectors. The signal is displayed using either a 0.5-GHz bandwidth (2 GS/s) or a 1-GHz bandwidth (5 GS/s) oscilloscope to monitor the overall pulse envelope. For a detailed study of the waveform of individual pulses, a 6-GHz bandwidth real-time oscilloscope was available. The overall response time of the electronic system was determined to be 100 ps.

II. Pulsed Operation

The absence of frequency-selective elements in the present cavity, together with the inherently broad-band nature of the intervalence band transition, causes laser action to occur simultaneously at a large number of longitudinal modes. Using a reflection grating in combination with a Schottky diode detector, the time- and wavelength-resolved optical output of the laser has been studied throughout the active region. Fig. 4 shows the E–B region of the present laser crystal for which laser action is observed. Due to the restrictions of the electro-magnet, observations were limited to fields up to 1.2 T. A separation into a low- and a high-field active region is clearly visible, both for $|E/B|$ values centered around 1.5 kV/cmT.

In Figs. 5 and 6, spectra recorded at a number of magnetic fields are shown in both the low- and high-field active regions,

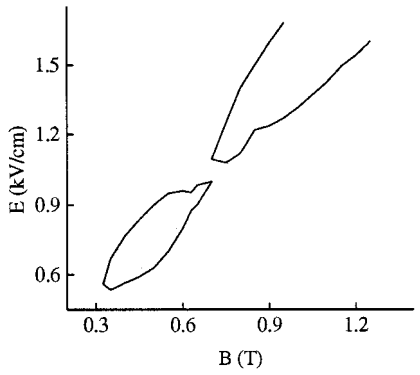

Fig. 4. E–B active region for the present laser crystal.

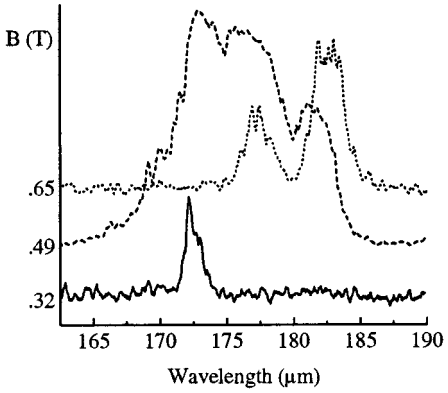

Fig. 5. Emission spectra in the low-B-field region.

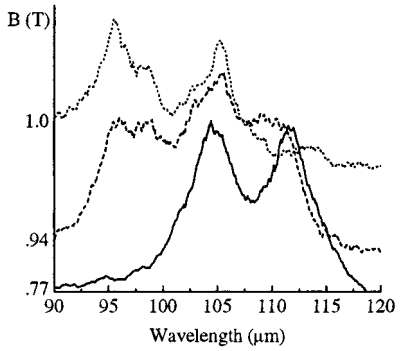

Fig. 6. Emission spectra in the high-B-field region.

respectively. Whereas for $B \geq 0.65$ T, the frequencies of the emission band tend to increase with increasing magnetic field, for the low-field region, the opposite seems to be the case. In Fig. 7, the overall range of emission frequencies as a function of the applied B-field is shown for normal pulsed operation. The frequency boundaries indicate the extrema that can be obtained also varying the amplitude of the E-field. The gap in the laser emission spectrum around 75 cm^{-1} is common for Ge : Ga hot hole lasers and is due to optical absorption by the Ga impurities. [8]. In the low-field range and in the lower part of the high-field range, the radiation is found to be polarized parallel to the magnetic field. For $B \geq 0.8T$, a small component $\| \vec{E}$ also develops, which increases in intensity toward larger E- and B-fields. This phenomenon is similar to what was reported by Hosako *et al.* for their Ge : Ga laser in a Voigt configuration [10].

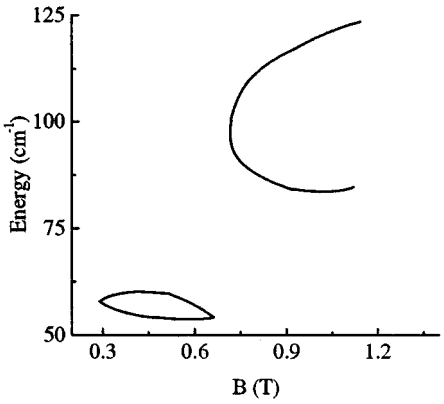

Fig. 7. Frequency band as a function of applied B-field.

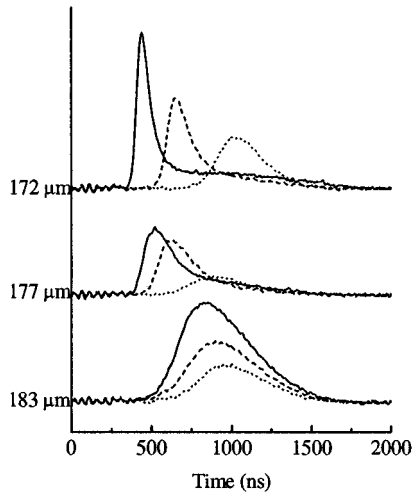

Fig. 8. Shape of the optical pulses for $B = 0.5$ T at three wavelengths, as a function of initial crystal temperature (see text for further explanation).

The general shape of the spectra recorded in the high-field region of this Ge : Ga laser can be understood using the arguments put forward by Reichertz *et al.* [9]. In Fig. 6, a structure of broad peaks with a mutual separation of about 10 cm^{-1}/T can clearly be observed. These peaks form a sequence of "allowed" and "spin–flip forbidden" transitions between subsequent LH Landau levels and the HH band. Increasing the E-field at constant B causes a change of the relative intensities of these peaks in a way similar to that described in [9].

The optical output in the low- and the high-field region has been observed both time and wavelength resolved. For $B = 0.5$ T, the pulseshapes at three different wavelengths are shown by the solid curves in Fig. 8. The zero of the time scales coincide with the moment that the approximately 3-μs-long E-field pulse reaches the necessary amplitude for laser action to occur. Emission in a broad band occurs, but laser action starts at the short wavelength (high energy) part of the spectrum whereas, during the pulse, longer wavelength components develop. At the end of the optical pulse, simultaneous emission across the total wavelength band occurs. From shot to shot, the relative intensities at these three wavelengths varies considerably, most probably due to longitudinal mode competition effects. However, the time delay versus wavelength remains quite constant. From the growth of inten-

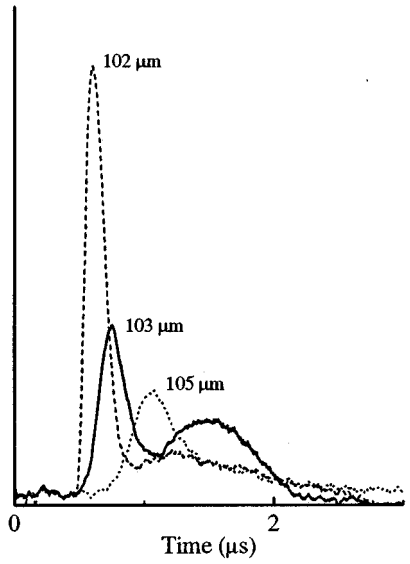

Fig. 9. Shape of the optical pulses for $B = 0.9$ T at three wavelengths.

sity in the early part of these pulses, the wavelength-dependent small-signal gain $g_{(\lambda)}$ has been determined to be $g_{(172)} = 0.015$ cm^{-1}, $g_{(177)} = 0.0026$ cm^{-1} and $g_{(182)} = 0.0021$ cm^{-1}. It must be noted that these values represent the *effective* gain, i.e., the actual (bare) gain reduced by, among others, reflection and outcouple losses. As these losses may well be in the order of 0.01 cm^{-1}, the wavelength dependence of the *bare* small-signal gain may not be as strong as the above values suggest.

As can be seen, the laser emission stops long before the end of the laser excitation. This is related to the strong heating of the crystal during excitation, which causes the laser gain to drop with time as a result of increasing lattice absorption and LH phonon scattering [11].

To study the influence of lattice heating on the emission, a two-pulse excitation experiment has been carried out. The first E-field pulse, with a low enough amplitude to avoid laser action, heats up the crystal. By applying the second pulse at a well-defined time delay after the first one, the initial lattice temperature of the crystal, at the moment of genuine laser excitation, can be increased in a controlled way. The solid curves in Fig. 8 have been taken at an initial temperature of $T = 4.2$K (liquid helium). The dashed–dotted and dotted curves were measured at higher initial lattice temperatures using this technique. Not unexpectedly, the time delay between excitation and start of laser emission increases and the small-signal gain and peak intensity decrease with increasing temperature for all three wavelengths. However, the amount of change differs with the result that, at higher initial lattice temperature, laser action starts at the *long* wavelength side of the spectrum.

In the high-field region, effects similar to those found in the low-field region are observed. In general, the small-signal gain is found to be larger, and laser action can be sustained for a somewhat longer period, despite the fact that, in this field region, the power dissipation is much larger because of the larger amplitude required for the excitation field. Fig. 9 show a typical results on the pulseshapes for three wavelengths at an initial temperature of $T = 4.2$K. In this particular case, the intensity at $\lambda = 103$ μm shows two peaks as a function of time; clearly, some sort of mode competition with the 105-μm component occurs. In this shorter wavelength region, the delay of laser action does not depend in a simple way on the wavelength, as in the case of the low-field region. In many circumstances, laser action starts at an intermediate wavelength, with contributions at both shorter and longer wavelength developing after some time. In view of the temperature dependencies of the delay times shown in Fig. 8, this effect may very well be related to the occurrence of a higher lattice temperature in this high-field active region. Quite often, the intensity of a wavelength component peaks more than once during a pulse. Moreover, in the case of a (relatively) large small-signal gain, intensity oscillations on a time scale of 15–40 ns are observed.

The origin of the above described effects is not clear; a further study along these lines might yield valuable information regarding the laser processes which, until now, are still largely unknown. However, the nature of the pulse-to-pulse variations of relative intensities for the different wavelengths, together with the odd temperature-dependent effects, suggest that the optical pumping mechanisms, as proposed in [12], are rather unlikely. They also seem to contradict the supposed homogeneous character of the intervalence band transition [13].

III. Mode-Locked Operation

With the modulation field $\vec{E}_\nu \parallel \vec{B}$ applied, active mode locking of the laser is achieved [6], [7]. Both in the low- and high-field regions, the overall wavelength ranges are slightly smaller and the time delays slightly larger than observed for pulsed operation. This is possibly related to the disturbing effect of the RF modulation field on the start of laser action. We observed that a short RF burst applied *before* the start of the high-voltage excitation, causes an additional delay of normal pulsed laser action. The magnitude of this delay depends on the intensity and duration of the RF burst and on the time interval between the end of the burst and the start of the high-voltage excitation pulse. A simple order of magnitude estimate shows that the observed delay is much too large as to only be the result of local heating effects of the crystal near the RF electrodes. We also found that the precise starting time of the RF pulse appears to be of great importance to obtain optimum mode-locked laser action. The origin of these effects is not clear at the moment; possibly, the impact ionization induced by the RF field creates an RF current path that counteracts the later formation of a homogeneous high-voltage current needed to obtain a proper population inversion.

In the upper trace of Fig. 10, the typical time-dependent optical output, as recorded with a 1-GHz bandwidth oscilloscope, under mode-locked conditions at $B = 0.5$ T is shown. A strongly amplitude modulated signal is observed, with a modulation frequency equal to the cavity round-trip frequency of 772 MHz. A wavelength-resolved inspection of this output reveals that only at the short wavelength side of the emission band—i.e., $\lambda \approx 172$ μm—the depth of modulation is nearly 100%. The longer wavelength components show a much smaller modulation. By comparing the wavelength-dependent pulseshapes (solid lines) in Fig. 8 with the "unmodulated"

Fig. 10. Optical output of mode locked laser for $B = 0.5$ T. Upper trace: active mode locking, lower trace: self-mode locking.

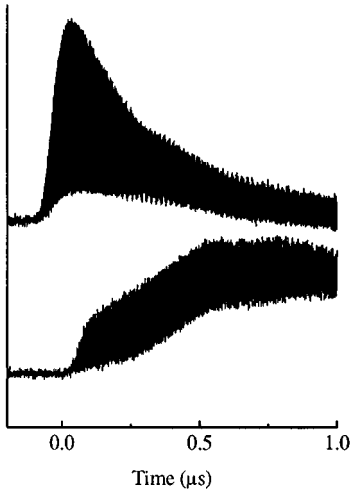

Fig. 11. Optical output of the active-mode-locked laser for $B = 0.9$ T at $\lambda = 97\ \mu$m (upper trace) and $\lambda = 108\ \mu$m (lower trace).

part of the upper trace in Fig. 10, it can also be concluded that the longer wavelength components are only weakly amplitude modulated. The lower trace in Fig. 10 is taken *without* application of RF modulation. The clearly visible 772-MHz modulation is due to "self mode locking" [7]. This self-mode-locking effect was found to occur in about 10% of the pulses in the low-field region.

In the high-field region, similar problems with the optical output under active-mode-locking conditions occur. In Fig. 11, the time-resolved output at $B = 0.9$ T is shown: at $\lambda = 97\ \mu$m (upper trace), the signal is strongly modulated. At $\lambda = 108\ \mu$m (lower trace), the intensity in the early part of the pulse is well modulated, but the modulation depth decreases strongly during the pulse. Using the 6-GHz bandwidth real-time oscilloscope, the output of the mode-locked laser has been studied with a much better time resolution. In the early stage of laser action (Fig. 12), a regular train of pulses with a 1.3-ns separation, i.e., the cavity round-trip time, is observed. The increase of intensity of successive pulses reflects the small-signal gain per cavity round trip

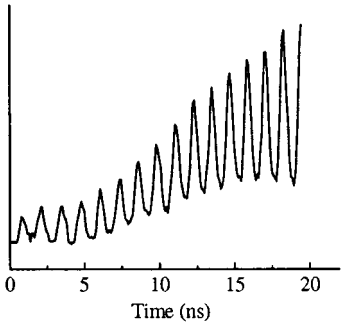

Fig. 12. Mode-locked laser output for $\lambda \approx 172\ \mu$m in the early start of laser action.

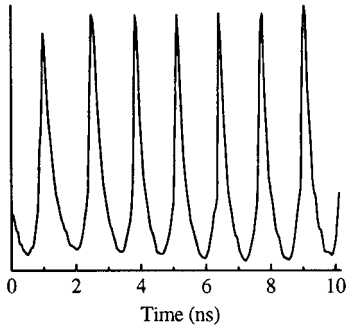

Fig. 13. Pulse train in saturated gain region for $\lambda \approx 172\ \mu$m.

of the optical pulse. Also, a decrease of pulsewidth, typical for the buildup period of mode-locked operation, is observed. The small-signal gain is found to be slightly larger than for normal pulsed operation at equal E and B fields. The RF field probably causes a loss of gain in that part of the crystal that is situated in between the modulation electrodes, i.e., in 20% of the overall length of the active medium. This conclusion is corroborated by the observation that, under otherwise equal conditions, without the RF modulation applied, the small-signal gain in the case of self-mode-locked operation can be nearly twice as large [7].

The slightly larger round-trip gain under actively mode-locked conditions clearly shows that the optical pulse does experience a larger gain in the unmodulated part of the crystal than the quasi-CW small-signal gain, as observed for normal pulsed operation. That suggests that the lifetime of the induced population inversion in that part of the crystal is a nonnegligible fraction of the 1.3-ns-cavity round-trip time.

Under saturated gain conditions, a train of constant-amplitude narrow pulses is observed (see Fig. 13). In the low-field region, the minimum width of these pulses is found to be about 100-ps FWHM. The electronic rise time of the detection system—Schottky diode, bias-T, and amplifiers—has been determined to be about 100 ps. It is, therefore, conceivable that the actual minimum width of the pulses may even be shorter. In the high-field regime, up until now, a minimum pulsewidth of 140 ps has been measured, using a different Schottky diode detector. In Fig. 14, a single micro pulse is shown with an even better time resolution. The wiggles in the tail of the signal are the result of internal reflections in the detector unit due to a slight impedance mismatch.

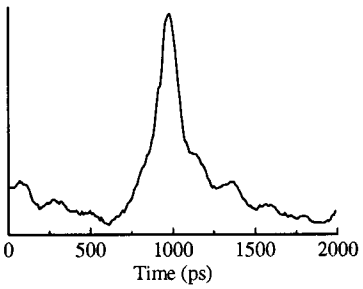

Fig. 14. Shape of micropulse in saturated gain region.

It must be noted that the mode-locked pulses depicted in Figs. 12–14 represent the "best typical" results. Due to the variation of emission wavelengths during laser action, stationary mode locking will strongly be hindered. To discuss these effects, we consider the best studied region around $\lambda = 172\ \mu$m.

Similar as for long-pulsed operation, also under active gain modulation, the laser action in the 177–182-μm region is delayed with respect to that in the 172-μm region. The much smaller gain at these wavelengths is lowered even more by the disturbing effect of the RF modulation field. As a consequence, no genuine mode locking is observed for that wavelength region. Only a low-intensity amplitude-modulated output is seen, without the above-described clear mode-locking characteristics. As a result, from the additional lowering of the gain in the long wavelength region, due to the modulation field, proper mode-locked action at 172 μm is sustained longer than would be expected from the time-resolved experiments under long pulsed operation. Nevertheless, in general, the duration of a properly behaving pulse train is only of the order of a few hundred nanoseconds.

In the high-field region, similar effects occur. However, due to the even more complicated time dependence of the emission frequencies, a well-behaving pulse train can only be produced by very carefully choosing the external lasing conditions.

IV. Conclusion

The results of a time- and wavelength-resolved study of the optical output of the mode-locked p-Ge hot hole laser, emitting in the terahertz range, has been reported in this paper. The system is able to produce trains of 100-ps FWHM pulses, yet the uncontrolled time-dependent variation of the emission wavelength *during* the laser excitation causes considerable problems. Possibly the introduction of a wavelength selective element in the cavity can lead to a better controlled output of the system.

Acknowledgment

This work is part of the Research Program of the European TMR Network "InterEuropean Terahertz Action (INTERACT)." The authors thank M. J. W. Vermeulen, Delft Interfacultary Reactor Institute, Delft, The Netherlands, for the use of the 6-GHz oscilloscope and help with the data acquisition.

References

[1] E. Gornik and A. A. Andronov, Eds., *Optical Quantum Electronics*. London: Chapman and Hall, 1991.

[2] E. Bründermann, A. M. Linhart, H. P. Röser, O. D. Dubon, W. L. Hansen, and E. E. Haller, "Miniaturization of p-Ge lasers: Progress toward continuous wave operation," *Appl. Phys. Lett.*, vol. 68, pp. 1359–1361, 1996.

[3] E. Bründermann, A. M. Linhart, L. A. Reichertz, H. P. Röser, O. D. Dubon, G. Sirmain, W. L. Hansen, and E. E. Haller, "Double acceptor doped Ge: A new medium for inter-valence-band lasers," *Appl. Phys. Lett.*, vol. 68, pp. 3075–3077, 1996.

[4] E. Bründermann, D. R. Chamberlain, and E. E. Haller, "Thermal effects in widely tunable germanium terahertz lasers," *Appl. Phys. Lett.*, vol. 73, pp. 2757–2759, 1998.

[5] R. C. Strijbos, J. G. S. Lok, and W. T. Wenckebach, "A Monte Carlo simulation of mode-locked hot-hole laser operation," *J. Phys. Condens. Matter*, vol. 6, pp. 7461–7468, 1994.

[6] J. N. Hovenier, A. V. Muravjov, S. G. Pavlov, V. N. Shastin, R. C. Strijbos, and W. T. Wenckebach, "Active mode locking of a p-Ge hot hole laser," *Appl. Phys. Lett.*, vol. 71, pp. 443–445, 1997.

[7] J. N. Hovenier, T. O. Klaassen, W. T. Wenckebach, A. V. Muravjov, S. G. Pavlov, and V. N. Shastin, "Gain of the mode locked p-Ge laser in the low field region," *Appl. Phys. Lett.*, vol. 72, pp. 1140–1142, 1998.

[8] W. Heiss, K. Unterrainer, E. Gornik, W. L. Hansen, and E. E. Haller, "Influence of impurity absorption on germanium hot-hole laser spectra," *Semicond. Sci. Technol.*, vol. 9, pp. 638–640, 1994.

[9] L. A. Reichertz, O. D. Dubon, G. Sirmain, E. Bründermann, W. L. Hansen, D. R. Chamberlain, A. M. Linhart, H. P. Röser, and E. E. Haller, "Stimulated far-infrared emission from combined cyclotron resonances in germanium," *Phys. Rev.*, vol. B56, pp. 12069–12072, 1997.

[10] I. Hosako and S. Komiyama, "p-type Ge far-infrared laser oscillation in Voigt configuration," *Semicond. Sci. Technol.*, vol. 7, pp. B645–648, 1992.

[11] S. Komiyama, S. Kuroda, I. Hosako, Y. Akasaka, and N. Iizuka, "Germanium lasers in the range from far-infrared to millimeter waves," *Opt. Quantum Electron.*, vol. 23, pp. S133–S162, 1991.

[12] S. V. Demihovsky, A. V. Murav'ev, S. G. Pavlov, and V. N. Shastin, "Stimulated emission using the tramsitions of shallow acceptor states in germanium," *Semicond. Sci. Technol.*, vol. 7, pp. B622–B625, 1992.

[13] F. Keilmann and R. Till, "Nonlinear far-infrared response of passive and active hole systems in p-Ge," *Semicond. Sci. Technol.*, vol. 7, pp. B633–B635, 1992.

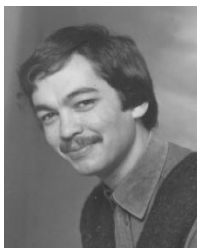

J. Niels Hovenier was born in Hilversum, The Netherlands. He received the degree in advanced electronic engineering from the School of Electronics, Hilversum, The Netherlands, in 1977.

From 1979 to 1990, he was an Electronic Engineer in the NMR Research Group, Physics Department, University of Leiden. Since 1991, he has been an Opto-Electronic Engineer with the Semiconductors Physics Group, Physics Department, Delft University of Technology, Delft, The Netherlands. He was involved in far infrared short-pulse/high-power pilot studies on semiconductors using the Dutch Free Electron Laser FELIX. His current research activities are in mode-locked p-Ge terahertz lasers and detection of short (picosecond) terahertz pulses.

M. Carmen Diez was born in Santander, Spain. She received the B.S. degrees in technical telecommunication engineer and telecommunication engineer from the University of Cantabria, Cantabria, Spain, in 1994 and 1997, respectively.

From October 1996 to July 1997, she was involved with the Final Career Project "Electromagnetic Models to Simulation of Indoor Radiopropagation," which was developed in the Communications Engineering Department, University of Cantabria. In 1997, she was a Graduate Assistant at the Direction of the School of Industrial and Telecommunication Engineering. Since January 1998, she has been a Graduate Research Assistant in the Department of Applied Physics, Delft University of Technology, Delft, The Netherlands. Her current research interests include semiconductors physics and far-infrared p-Ge lasers and submillimeter antireflection coatings.

Tjeerd O. Klaassen (A'95) received the M.Sc. and Ph.D. degrees in physics from the University of Leiden, Leiden, The Netherlands, in 1967 and 1973, respectively.

As staff member of the Physics Department, University of Leiden, he was involved in the study of low-dimensional magnetic systems using magnetic resonance and relaxation techniques. In 1985, he became involved in the field of far-infrared spectroscopy of impurities in semiconductors. Since 1990, he has been with the Department of Applied Physics, Delft University of Technology, Delft, The Netherlands, where he is involved in (non)linear far-infrared spectroscopy in semiconductors and the development of active (p-Ge laser) and passive (antennas, transmission lines) components for terahertz electronics.

W. Tom Wenckebach, photograph and biography not available at time of publication.

Andrej V. Muravjov, photograph and biography not available at time of publication.

Sergey G. Pavlov, photograph and biography not available at time of publication.

Valerie N. Shastin, photograph and biography not available at time of publication.